Pathway for the Strain-Driven Two-Dimensional to Three-Dimensional Transition during Growth of Ge on Si(001)

A. Vailionis, B. Cho, G. Glass, P. Desjardins, David G. Cahill, and J. E. Greene
Department of Materials Science and the Materials Research Laboratory, University of Illinois, 104 South Goodwin Avenue, Urbana, Illinois 61801
(Received 24 May 2000)

The two-dimensional (2D) to three-dimensional (3D) morphological transition in strained Ge layers grown on Si(001) is investigated using scanning tunneling microscopy. The initial step takes place via the formation of 2D islands which evolve into small ($\simeq$ 180 Å) 3D islands with a height to base diameter ratio of $\simeq$0.04, much smaller than the 0.1 aspect ratio of {105}-faceted pyramids which had previously been assumed to be the initial 3D islands. The "prepyramid" Ge islands have rounded bases with steps oriented along $\langle 110 \rangle$ and exist only over a narrow range of Ge coverages, 3.5–3.9 monolayers.

PACS numbers: 68.55.Jk, 81.15.–z

The growth of Ge layers on Si(001) has been a subject of intense interest for several years due primarily to the fact that Ge/Si(001) serves as a model system for studying the strain-driven transition, with increasing layer thickness, in surface morphology from smooth two-dimensional (2D) wetting layers to coherent (i.e., dislocation-free) self-organized three-dimensional (3D) islands [1]. While the ability to form dislocation-free Ge islands on Si(001) represents an important step toward the creation of coherently strained 3D device structures, understanding of the processes governing island self-ordering and size uniformity is still far from complete. Atomic-scale analyses of the early stages of the strain-induced 2D to 3D morphological transition may provide insights into factors controlling the nucleation and size distribution of coherent 3D islands.

The appearance of small Ge clusters prior to the formation of large islands was first reported by Mo *et al.* using scanning tunneling microscopy (STM) [2]. The small clusters are faceted square pyramids or elongated rectangular pyramids ("huts") bounded by {105} planes. Larger islands ("domes"), which form at later stages, are more rounded and bound by {113} and {15 3 23} facets [3]. The evolution from pyramids to domes has been studied intensively using STM and atomic force microscopy (AFM) [4,5], as well as theory [6]. However, experimental observations and theoretical predictions of the pathway for the strain-induced transition from the 2D wetting layer to faceted 3D pyramids are still subject to controversy.

It is generally assumed that for Ge/Si(001), the 4.2% misfit strain induces the spontaneous formation of 3D faceted pyramids after growth of a 3 to 4 monolayer (ML) thick 2D wetting layer. In contrast, 2D islands and quasi-3D clusters (6–12 Å high) have been observed by STM and reported as an intermediate state in the transition from the 2D wetting layer to 3D islands in the more highly strained InAs/GaAs(001) system (mismatch $\simeq$7%) [7]. Systematic growth and annealing studies of lower-strained $Si_{1-x}Ge_x$ alloys on Si(001) show that the 2D to 3D transition occurs via small islands and ripples which have aspect ratios smaller than those corresponding to {105}-faceted pyramids [8,9].

There have been some theoretical attempts to describe a possible gradual 2D to 3D transformation via precursors (e.g., 2D platelets) during highly mismatched heteroepitaxy [10]. However, until now, no experimental evidence has been reported for the existence of an initial "prepyramid" state in the 2D to 3D surface morphological transition in pure Ge layers on Si(001). The existence of an intermediate Ge morphological state between the 2D wetting layer and pyramid formation is difficult to test experimentally at high misfit strains ε_0 where the driving force for island formation is large and the island size d, which scales as ε_0^{-2}, is small [9].

In this Letter, we present direct STM evidence for the existence of initial prepyramid roughening states in Ge epitaxial layers grown on Si(001) at 650 °C. The prepyramid islands, which exhibit rounded bases, serve as precursors for the formation of the larger {105}-faceted, $\langle 100 \rangle$ square-based, pyramids.

The substrates for Ge/Si(001) growth were n-type Si(001) wafers with a miscut of 0.3° toward [110] as measured by STM. Following substrate cleaning [11], an $\simeq$500 Å thick Si buffer layer was grown in an ultrahigh vacuum multichamber gas-source molecular beam epitaxy (GS-MBE) system from Si_2H_6 at 800 °C. This resulted in STM images exhibiting clean Si(001) surfaces consisting of monatomic height steps arranged along [110] with average terrace sizes of 300 Å. Ge/Si(001) samples with Ge coverages θ_{Ge} ranging from 2 to 12 ML were grown at 650 °C using a Ge_2H_6 flux of 2.8×10^{14} cm^{-2} s^{-1} which provided a deposition rate of 1.8 ML min^{-1} as determined by Rutherford backscattering spectrometry. The Ge growth temperature is well above the monohydride desorption temperatures, 290–340 °C for Ge(001) and 500–550 °C for Si(001) [11]. Following Ge deposition, the sample was immediately quenched at a rate of $\simeq$100 °C s^{-1} and transferred *in situ* into the STM chamber.

 0031-9007/00/85(17)/3672(4)$15.00

Figure 1 shows STM images of Ge(001) layers with coverages θ_{Ge} between 2.8 and 4.0 ML. For $\theta_{Ge} < 3.0$ ML, the Ge layer is fully two dimensional. The first observed surface structural transition is a change in surface reconstruction from 2×1 to $2 \times N$ which occurs at $\theta_{Ge} \simeq 1$ ML due to the introduction of dimer vacancy lines (DVL) [12,13], where N corresponds to the number of dimer rows between the DVLs. With further Ge deposition, the periodicity N decreases in order to relieve the increasing strain. However, because of the short-range repulsive interaction between dimer vacancies, the maximum N value is approximately 8 and this occurs at $\theta_{Ge} \simeq 1.6$–2.1 ML [13]. At higher Ge coverages, there is a second strain-driven surface structural transition, $2 \times N \rightarrow M \times N$ as dimer row vacancies (DRV), of width M rows, form perpendicular to the original DVLs [12]. The $M \times N$ surface morphology at $\theta_{Ge} = 2.8$ ML is shown in Fig. 1(a) to consist of a 2D grid defined by orthogonal DVLs and DRVs.

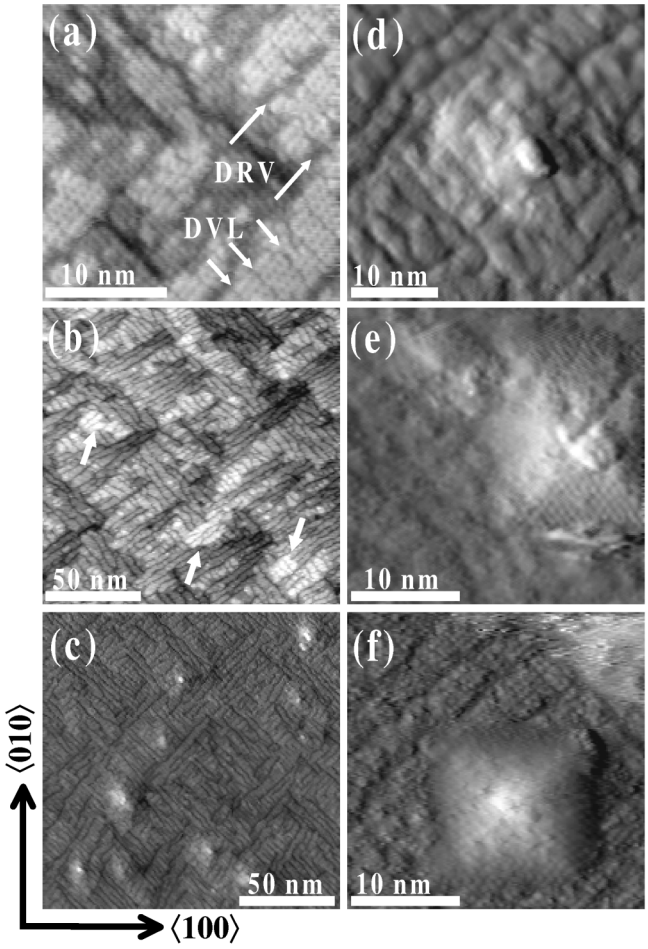

FIG. 1. STM images showing the evolution of Ge grown on Si(001): (a),(b) 2D wetting layer at $\theta_{Ge} = 2.8$ and 2.9 ML, respectively, (c) 3D prepyramid islands at $\theta_{Ge} = 3.55$ ML, (d) initial prepyramid island at $\theta_{Ge} = 3.55$ ML, (e) (001)-truncated {105}-faceted pyramid at $\theta_{Ge} = 3.85$ ML, and (f) completely formed {105}-faceted pyramid at $\theta_{Ge} = 4.0$ ML. DVL and DRV are dimer vacancy lines and dimer row vacancies, respectively. 2D islands in (b) are labeled with arrows. The images are partially differentiated to enhance the details and they appear sidelit from the lower left corner.

As deposition proceeds, the Ge surface begins to exhibit 1 ML height islands, labeled with arrows in Fig. 1(b), at $\theta_{Ge} = 2.9$ ML. Further Ge deposition, beyond 3.0 ML, leads to the formation of small 3D islands. Examples at a Ge coverage of 3.55 ML are shown in Fig. 1(c). Higher-resolution STM images of 3D islands formed at $\theta_{Ge} = 3.55$, 3.85, and 4.0 ML are presented in Figs. 1(d), 1(e), and 1(f), respectively. The image of the island in Fig. 1(d) was obtained from the sample corresponding to Fig. 1(c). In contrast to {105}-faceted pyramids with ⟨100⟩ oriented bases, previously reported to be the first 3D islands to form in Ge on Si(001), Figs. 1(c) and 1(d) show that the initial 3D Ge islands exhibit more rounded bases and are bounded by steps oriented approximately along ⟨110⟩. The aspect ratio (island height to width) of the initial 3D islands is $\simeq$0.04, much lower than that of {105}-faceted pyramids, which is typically 0.1 [2].

Further increases in Ge coverage lead to the formation of pyramids. Figure 1(e) shows a typical pyramid with a rectangular ⟨100⟩ base. At this coverage, $\theta_{Ge} = 3.85$ ML, the pyramid sides are truncated {105} facets with a flat (001) top containing dimer vacancy lines, similar to those in the wetting layer [Fig. 1(a)]. As growth continues, the truncated structures eventually develop into complete pyramids such as the one shown in Fig. 1(f) ($\theta_{Ge} = 4.0$ ML) with an inclination angle of $11° \pm 0.4°$ close to that of a perfect {105} facet, 11.3°. At even higher Ge coverages, AFM images show that pyramids coexist with dome-shaped islands. It is important to note that pyramid size distributions are bimodal: small pyramids with base diameters $d \leq 300$ Å and larger pyramids with $500 \leq d \leq 700$ Å. Our high coverage ($\theta_{Ge} > 4.0$ ML), large-scale features are consistent with surface morphologies of previously reported Ge layers grown by solid-source MBE on Si(001) at $T_s = 600$ °C where the size of the larger pyramids was attributed to Ge/Si alloying [14].

We plot the number density n of 3D prepyramid islands, small pyramids, large pyramids, and domes as a function of θ_{Ge} in Fig. 2. The prepyramid island densities were obtained from STM images while pyramid and dome densities at coverages $\theta_{Ge} > 4$ ML were obtained from AFM images. The prepyramid islands are observed only over a very narrow Ge coverage which, for the growth conditions used here, ranges from 3.5 to 3.9 ML. At higher coverages, small and large pyramids, as well as domes, appear essentially simultaneously. As can be seen from Fig. 2 the prepyramid island density at $\theta_{Ge} = 3.9$ ML ($n \simeq 1.3 \times 10^{10}$ cm^{-2}) and the density of small pyramids at $\theta_{Ge} = 4.1$ ML ($n \simeq 1.4 \times 10^{10}$ cm^{-2}) are approximately equal, suggesting that prepyramids act as precursors for the formation of small {105}-faceted pyramids. For Ge coverages $\theta_{Ge} = 5.4$–12 ML only domes, with number density $n \simeq 10^9$ cm^{-2}, are observed.

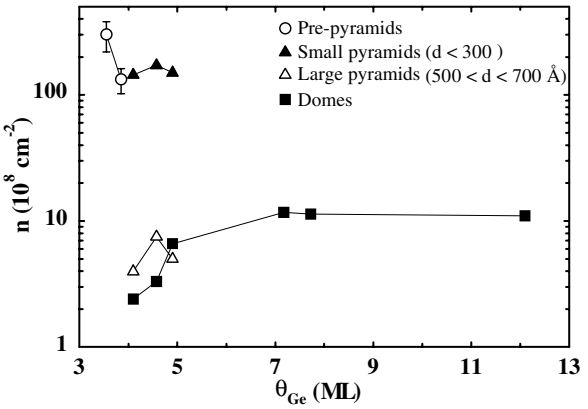

FIG. 2. Number density n of prepyramid islands, small {105}-faceted pyramids, large {105} pyramids, and domes as a function of Ge coverage θ_{Ge} on Si(001). The prepyramid island densities were obtained from STM images, while n values for small and large pyramids and domes were obtained from AFM scans. The STM detection limit for prepyramids corresponds to $n \simeq 3.5 \times 10^8$ cm^{-2} and the AFM detection limit is 2.5×10^7 cm^{-2}.

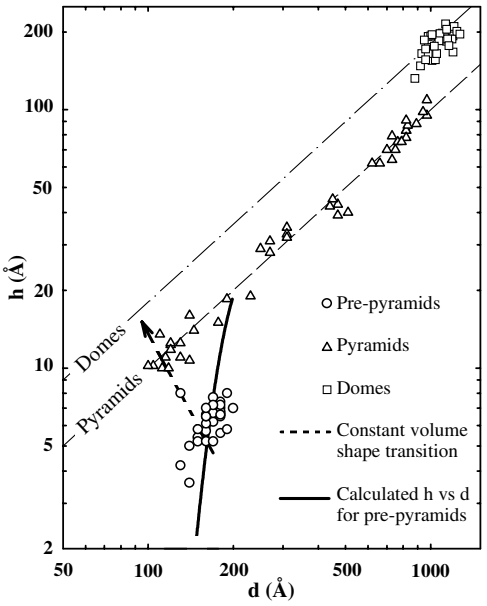

FIG. 3. Height h of 3D prepyramid islands and {105}-faceted pyramids as a function of lateral size d in GS-MBE Ge grown layers on Si(001). Dashed and dot-dashed lines correspond to the height-to-width aspect ratios of {105} pyramids ($h/d = 0.1$) and domes ($h/d = 0.18$), respectively. The arrow represents a constant volume shape transition of prepyramids to {105}-faceted pyramids. The solid line corresponds to the calculated island height as a function of island diameter (see text).

Based upon the above results, we propose that the transition from a 2D Ge wetting layer on Si(001) to coherent dome clusters occurs through the following steps: the growth of a 2D wetting layer, formation of 2D islands, small (130–200 Å) nonfaceted 3D islands (prepyramids with rounded bases), a bimodal distribution of {105}-faceted pyramids with ⟨100⟩ bases, pyramids coexisting with dome-shaped clusters, and, finally, just domes.

The growth of lower-strain $Si_{0.8}Ge_{0.2}$ layers on Si(001) also exhibits a complex multistep 2D to 3D transition [9], but one which is much different than that reported here for the higher-strain Ge/Si(001) case. The earliest 3D islands observed in MBE $Si_{0.8}Ge_{0.2}$ layers grown at 760 °C are small rounded nonfaceted features which occur at $\theta_{\mathrm{Ge}} \simeq 18$ ML with average size $d \simeq 3000$ Å followed by the formation of a ripple structure along orthogonal ⟨100⟩ directions rather than discrete 3D islands [9]. For $Si_{0.8}Ge_{0.2}$/Si(001), the lattice misfit strain $\varepsilon = 0.0084$ compared to 0.042 for Ge/Si(001). Since the initial island size d scales with ε^{-2} [9] and measured d values for $Si_{0.8}Ge_{0.2}$/Si(001) are ≃3000 Å, the initial 3D island size extrapolated to pure Ge on Si(001) is ≃120 Å, in good agreement with the smallest prepyramids we observe, 130 Å.

Figure 3 is a plot of the height h vs size d of 3D prepyramid islands showing that their height-to-width ratio varies from 0.03 to 0.05 with increasing island size. In contrast, we, as well as previous investigators [2–5], observe that {105}-faceted Ge pyramids on Si(001) exhibit an aspect ratio of 0.1 which remains approximately constant as the pyramid size increases. The aspect ratio of prepyramids increases with island size until at $d \simeq 160$–200 Å, they transform into {105}-faceted ⟨100⟩ oriented pyramids.

Analyses of our STM images suggest that the transformation from prepyramids to pyramids takes place at approximately constant volume through rearrangement of Ge atoms in the island such that the island width d decreases while the height h increases as $h \propto d^{-2}$.

The constant-volume shape transition trajectory, shown as a dashed line in Fig. 3, is consistent with our experimentally observed island sizes. In our volume estimations, we use aspect ratios determined from STM images and the fact that the prepyramids are approximately pyramidal (volume $= hd^2/3$) in shape. The error in this approximation is ≤15% [15]. Once prepyramid islands transform into {105}-faceted pyramids, the aspect ratio stabilizes at 0.1 and further growth occurs via a continuous volume increase while maintaining a self-similar shape up to the pyramid-to-dome transition.

The initial strain-driven roughening leading to prepyramid formation during Ge/Si(001) growth can be modeled using theoretical approaches where the large-scale surface morphology is approximated by a periodic array of small 3D islands on an otherwise flat surface [16,17]. Kukta *et al.* [17] calculated surface morphological evolution for epitaxial islands assuming that the total free energy of the system consists of only an isotropic surface energy and the elastic energy. Since our low-aspect-ratio prepyramids do not contain well-defined facets, the assumption of an isotropic surface energy [17] appears reasonable. They [17] show that the equilibrium volume of a 3D island is

a function of a single characteristic length L, which for biaxial misfit strain is $L = [\sqrt{2}/(1 + \nu)]\gamma/E\varepsilon^2$ [18], where γ is the surface energy, ν is the Poisson ratio, and E is the plane strain modulus. Substituting parameters appropriate for Ge/Si(001)—$\gamma = 1\ \mathrm{J\,m^{-2}}$ [19], $E = 1.3 \times 10^{11}$ Pa, $\varepsilon = 0.042$, and $\nu = 0.275$—yields $L = 50$ Å. Combining this result with the calculated dependence of the aspect ratio h/d vs normalized island area A/L^2 (Ref. [17]), we obtain a relationship, with no free parameters, for the equilibrium island size and shape. The calculated h vs d dependence shown in Fig. 3 as a solid line exhibits good agreement with our experimental data for the prepyramids with island sizes $d \lesssim 200$ Å.

In the above h vs d calculations, we used a mismatch strain ε appropriate for pure Ge islands, while it is known that intermixing between the Ge overlayer and the Si substrate can occur at our growth temperature, 650 °C [14]. Indeed, large dome clusters with diameters of approximately 1000 Å in our Ge overlayers had average compositions near $Ge_{0.85}Si_{0.15}$ as deduced from strain relaxation within the dome measured by transmission electron microscopy using two-beam dark-field strain imaging [20]. However, prepyramid compositions cannot be derived directly from the Ge/Si ratio observed in domes. Studies of strain-driven alloying in MBE-grown Ge/Si(001) islands by Chaparro *et al.* [14] show that the size distribution of {105}-faceted pyramids with diameters $d \leq 250$ Å does not change with growth temperature over the range 450–600 °C, but that there are significant size variations in large pyramids ($500 \leq d \leq 700$ Å) and domes ($700 \leq d \leq 900$ Å). These results suggest that measurable alloying of Ge pyramids requires significant incubation time after nucleation. For MBE Ge grown on Si(001) at $T_s = 300$ °C where Si/Ge intermixing is negligible, the size of the smallest {105}-faceted pyramids observed by Jesson *et al.* are about 130 Å [21], approximately the same size as our small pyramids grown at $T_s = 650$ °C. This suggests that our small pyramids and prepyramids do not contain a significant concentration of Si.

In summary, we have used *in situ* STM to determine the initial stages in the 2D to 3D morphological transition for Ge layers grown on Si(001). We demonstrate that the first step following the $2 \times 1 \rightarrow 2 \times N$ ($\theta_{\mathrm{GE}} \simeq 1$ ML) $\rightarrow$ $M \times N$ ($\theta_{\mathrm{Ge}} \simeq 1.6$ ML) surface structural transitions is the formation of atomically flat 2D islands which evolve into small ($d = 130$–200 Å) nonfaceted rounded 3D islands with aspect ratios of 0.03–0.05 over a narrow range of Ge coverages, 3.5–3.9 ML. These prepyramids have steps along ⟨110⟩ and their aspect ratios increase from 0.03 at $d = 130$ Å to 0.05 at $d = 200$ Å. As the Ge coverage is increased beyond 4.0 ML, prepyramid islands transform into {105}-faceted pyramids with ⟨100⟩ oriented rectangular bases and an aspect ratio of $\simeq$0.1 irrespective of pyramid size. The prepyramid to pyramid transition occurs at constant volume through rearrangement of Ge atoms such that d decreases while the height h increases as $h \propto d^{-2}$.

The authors gratefully acknowledge the financial support of the U.S. Department of Energy, Division of Materials Sciences, under Contract No. DEFG02-ER9645439 and NSF Division of Materials Research Grant No. DMR 97-05440. We thank Dr. Chuan-Pu Liu for the TEM measurements. P. D. is partially supported by NSERC (Canada).

[1] D. J. Eaglesham and M. Cerullo, Phys. Rev. Lett. **64**, 1943 (1990).
[2] Y.-W. Mo *et al.,* Phys. Rev. Lett. **65**, 1020 (1990).
[3] F. M. Ross, R. M. Tromp, and M. C. Reuter, Science **286**, 1931 (1999).
[4] M. Tomitori *et al.,* Appl. Surf. Sci. **76/77**, 322 (1994).
[5] G. Medeiros-Ribeiro *et al.,* Science **279**, 353 (1998).
[6] J. Tersoff and F. K. LeGoues, Phys. Rev. Lett. **72**, 3570 (1994); V. A. Shchukin *et al.,* Phys. Rev. Lett. **75**, 2968 (1995); I. Daruka and A.-L. Barabási, Phys. Rev. Lett. **79**, 3708 (1997); H. T. Dobbs *et al.,* Phys. Rev. Lett. **79**, 897 (1997).
[7] R. Heitz *et al.,* Phys. Rev. Lett. **78**, 4071 (1997).
[8] A. J. Pidduck *et al.,* Thin Solid Films **222**, 78 (1992); K. M. Chen *et al.,* Phys. Rev. B **56**, R1700 (1997).
[9] J. A. Floro *et al.,* Phys. Rev. B **59**, 1990 (1999).
[10] C. Priester and M. Lannoo, Phys. Rev. Lett. **75**, 93 (1995); Y. Chen and J. Washburn, Phys. Rev. Lett. **77**, 4046 (1996).
[11] H. Kim and J. E. Greene, J. Vac. Sci. Technol. A **17**, 354 (1999); H. Kim *et al.,* J. Appl. Phys. **82**, 6062 (1997).
[12] I. Goldfarb *et al.,* Surf. Sci. **394**, 105 (1997).
[13] F. Wu *et al.,* Phys. Rev. Lett. **74**, 574 (1995); B. Voigtländer and M. Kästner, Phys. Rev. B **60**, R5121 (1999).
[14] S. A. Chaparro *et al.,* Phys. Rev. Lett. **83**, 1199 (1999).
[15] The actual shape of the 3D islands during the prepyramid to pyramid transition changes from cosinelike at aspect ratio $\simeq$0.04 to a complete {105}-faceted pyramid with aspect ratio = 0.1.
[16] H. Gao, J. Mech. Phys. Solids **39**, 443 (1991); B. J. Spencer and J. Tersoff, Phys. Rev. Lett. **79**, 4858 (1997).
[17] R. V. Kukta and L. B. Freund, J. Mech. Phys. Solids **45**, 1835 (1997).
[18] L. B. Freund (private communication).
[19] Zheng Gai *et al.,* Phys. Rev. B **59**, 15 230 (1999).
[20] Chuan-Pu Liu *et al.,* Phys. Rev. Lett. **84**, 1958 (2000).
[21] D. E. Jesson, M. Kästner, and B. Voigtländer, Phys. Rev. Lett. **84**, 330 (2000).